

Article

Impact of Climate and Land-Use Change on Groundwater Resources, Study of Faisalabad District, Pakistan

Meer Muhammad Sajjad ^{1,2}, Juanle Wang ^{1,2,3,4,*} , Haider Abbas ^{2,5}, Irfan Ullah ^{6,7} , Rehan Khan ⁸ 
and Furman Ali ^{2,9}

- ¹ State Key Laboratory of Resources and Environmental Information System, Institute of Geographic Sciences and Natural Resources Research, Chinese Academy of Sciences, Beijing 100101, China; meersajjad@igsnr.ac.cn
- ² University of Chinese Academy of Sciences, Beijing 100049, China; habbas@igsnr.ac.cn (H.A.); goldengeographer@mailsucas.ac.cn (F.A.)
- ³ China-Pakistan Earth Science Research Center, Islamabad 45320, Pakistan
- ⁴ Jiangsu Center for Collaborative Innovation in Geographical Information Resource Development and Application, Nanjing 210023, China
- ⁵ Key Laboratory of Ecosystem Network Observations and Modeling, Institute of Geographic Sciences and Natural Resources Research, Chinese Academy of Sciences, Beijing 100101, China
- ⁶ School of Atmospheric Sciences, Nanjing University of Information Science and Technology (NUIST), Nanjing 210044, China; irfan.marwat@nuist.edu.cn
- ⁷ Key Laboratory of Hydrometeorological Disaster Mechanism and Warning of Ministry of Water Resources, Nanjing University of Information Science and Technology, Nanjing 210044, China
- ⁸ Key Laboratory of Metallogenic Prediction of Nonferrous Metals and Geological Environment Monitoring, Ministry of Education, School of Geosciences and Info-Physics, Central South University, Changsha 410083, China; rehankhan@csu.edu.cn
- ⁹ State Key Laboratory of Remote Sensing Science, Aerospace Information Research Institute, University of Chinese Academy of Sciences, Beijing 100049, China
- * Correspondence: wangjl@igsnr.ac.cn; Tel.: +86-010-6488-8016



Citation: Sajjad, M.M.; Wang, J.; Abbas, H.; Ullah, I.; Khan, R.; Ali, F. Impact of Climate and Land-Use Change on Groundwater Resources, Study of Faisalabad District, Pakistan. *Atmosphere* **2022**, *13*, 1097. <https://doi.org/10.3390/atmos13071097>

Academic Editor: Hanbo Yang

Received: 21 June 2022

Accepted: 10 July 2022

Published: 13 July 2022

Publisher's Note: MDPI stays neutral with regard to jurisdictional claims in published maps and institutional affiliations.



Copyright: © 2022 by the authors. Licensee MDPI, Basel, Switzerland. This article is an open access article distributed under the terms and conditions of the Creative Commons Attribution (CC BY) license (<https://creativecommons.org/licenses/by/4.0/>).

Abstract: Groundwater depletion has become a major concern all over the world. Recently, the rapid population growth and need for water and food have placed a massive strain on land and water resources. In this study, groundwater depletion resulting from land-use and climate change was investigated in the Faisalabad district, Pakistan, from 2000 to 2015. A Pearson correlation analysis between climatic parameters and land-use indices with groundwater was conducted to explore the major influencing factors. Interpolation maps of groundwater were generated using the inverse distance weighting interpolation (IDW) method. The Normalized Difference Built-up Index (NDBI) of five-year intervals demonstrated a strong increasing trend, whereas the Normalized Difference Vegetation Index (NDVI) presented a declining trend. The results also indicated a significant declining trend in groundwater levels in the region, with the annual average groundwater level decreasing at a rate of approximately 0.11 m/year. Climatic parameters (i.e., precipitation and temperature) further reveal an insignificant increasing trend estimated using the Mann–Kendall test and Sens's slope. Overall, spatial analysis results showed a statistically significant positive trend in the groundwater level of the Faisalabad district, where the NDBI ratio is high and the NDVI is low, owing to the extensive extraction of groundwater for domestic and industrial use. These findings may be useful for a better understanding of groundwater depletion in densely populated areas and could also aid in devising safety procedures for sustainable groundwater management.

Keywords: groundwater; NDVI; NDBI; climate parameters; district Faisalabad; Pakistan

1. Introduction

Groundwater, an enormous freshwater reserve beneath Earth's surface, is an essential resource for humanity and ecosystems [1]. More than a third of the water consumed worldwide originates from underground sources, supplying approximately 42%, 36%, and

27% of the water used for agricultural, domestic, and industrial purposes, respectively [2]. It provides a huge amount of fresh water for drinking, agricultural, and industrial use worldwide [3,4].

Groundwater demand is rapidly increasing with the increase in human activities [5]. Rapid worldwide population growth has resulted in an overall increase in global water consumption, adding to the anthropogenic stress on water supplies [6]. The subject of how urbanization affects groundwater depletion has received extensive attention [7]. The urban expansion of human settlements and industrial development has affected urban growth patterns, resulting in the conversion of many fertile land surfaces into built-up regions [8]. Many business organizations and enterprises in various regions of the world use groundwater as well, especially for industries, such as paper, marble cutting, food, beverages, and other materials [9]. Climate change is adding to the strain on groundwater resources and increasing the risk of groundwater recharge. Droughts and climate variability have adversely affected food security, access to safe drinking water, hygiene, and public health [10]. Urban expansion and rural development can result in drought owing to over-pumping for daily use and industrial activities [9,11].

Groundwater use is one of the most important factors in urban development that potentially affects the groundwater ecosystem. Lack of reasonable land-use policies are contributing to the degradation of groundwater in developing countries, especially in city regions. In South Asia, major cities of countries such as Pakistan, India, and Bangladesh are experiencing population growth, drought, and heat wave disasters, leading to high stress on water resources [12–14]. These increasing urbanization trends are enforcing groundwater consumption in the region. An effective land-use management system for urban development concerned with groundwater could aid in the restoration of the quality of life and water resources. A lack of information on changes in groundwater storage hinders the development and implementation of effective water management plans [15]. Thus, evaluating the impact of climate and land-use on groundwater resources is necessary.

Previous studies have offered frameworks for assessing changes in groundwater resources. A recent study [16] on the impacts of climate on water resources reported that water yield, especially that controlled by evapotranspiration (ET) and precipitation, as well as land-use cover change caused by the human population, may indirectly affect available water resources. According to another study [17], groundwater recharge is affected by land-use change caused by anthropogenic activities, which also have a significant impact on groundwater flow dynamics. According to one study in Cambodia [18], precipitation and temperature also cause significant changes in groundwater. The higher the precipitation, the higher the potential recharge of groundwater; however, the rapid pace of urbanization, along with climate change, has substantially impacted surface and groundwater flows. Several studies [19–24] have been conducted using the SWAT model to investigate the response of hydrological variables to land-use change and climate variability in a watershed. Other researchers [7,25–30] have observed that the effect of land-use and climate changes on groundwater is a major issue worldwide. Different techniques, such as chloride mass balance (CMB) techniques and empirical methods, can be used to monitor the effect of land-use and climate changes on regional groundwater [31]. Among various methods, remote sensing is a suitable technique for monitoring large areas while minimizing the time and money spent for collecting data, particularly to analyze the impact of land-use change on groundwater [32]. This has enabled large-scale studies for providing information about land degradation and variations in groundwater to city planners.

Faisalabad, the third-largest city of Pakistan, is located in the central region of Pakistan between the high Asia region of the Tibetan Plateau and the low coastal region of the Arabian Sea. Its population has dramatically increased in recent years and has now become a serious problem. As the agricultural zone shrinks, the pattern of land-use constantly changes in urban regions. The increasing population, in both urban and rural parts of the Faisalabad district, relies on groundwater [33]. Faisalabad district is thus experiencing

significant groundwater depletion as a result of substantial groundwater extraction and rapidly growing urban areas.

The objective of this study is to examine the impacts of land-use changes and climate change on groundwater in the Faisalabad district from 2000 to 2015 using remote sensing data and field measurements of groundwater wells. The findings of this study can provide an understanding of the impact of land-use change and climatic variability on groundwater resources. Therefore, the study is essential for city planners, municipality experts, the irrigation department, as well as other governmental officials, for making climate adaptation plans in the region.

2. Materials and Methods

2.1. Study Area

This research was conducted in the industrial city of the Faisalabad district, Pakistan ($31^{\circ}25'15.7620''$ N, $73^{\circ}5'21.4584''$ E) (Figure 1). The plain fields of Faisalabad are mostly situated on the upper east side of Punjab, with a height of 184 m above sea level [34]. Faisalabad district has a total area of 5856 km², where Faisalabad city occupies an area of more than 200 km². There are eight towns in the district, namely Lyallpur, Jinnah, Iqbal, Madina, Chak Jhumra, Sammundri, Jaranwala, and Tandlianwala (Figure 1).

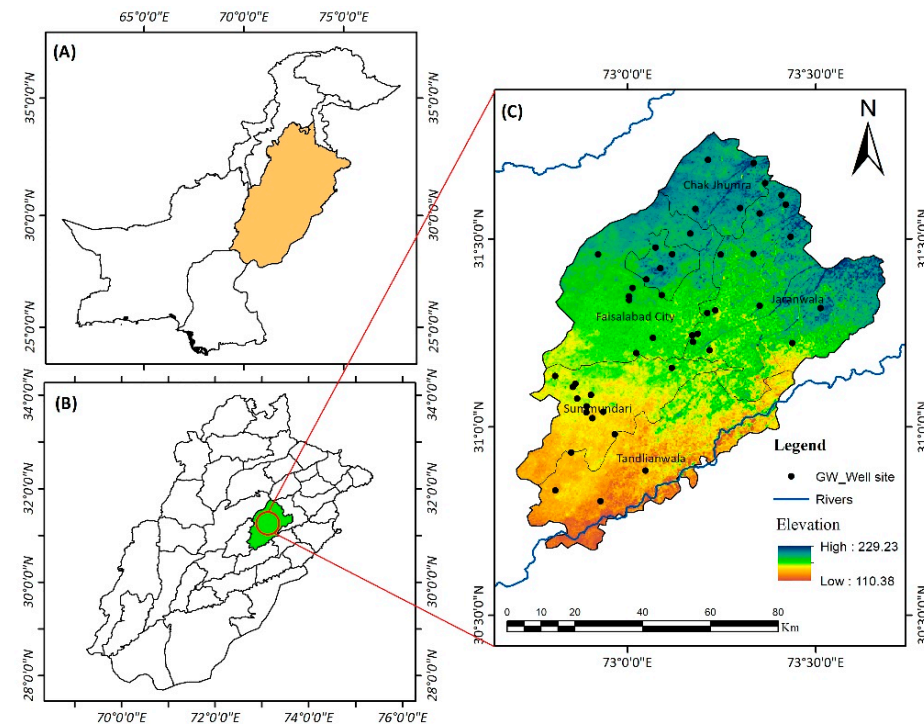


Figure 1. Location of the study area and the administrative boundaries of Pakistan (A), Panjab province (B), and Faisalabad district (C).

In 1901, Faisalabad had a population of 9171 people, which grew to 70,000 in 1941 and 179,000 in 1951, after the partition of Pakistan. After ten years, this number reached 425,000. According to the Pakistan Bureau of Statistics, the population increased to approximately 5.43 million in 1998, and it exceeded 7.88 million in 2017 [35]. The lower Chenab canal is an important water source infrastructure responsible for the irrigation of 80% of the cultivated fields in the study area. Faisalabad rests on alluvial loess soils with calcareous characteristics, rendering the region extremely productive. The Chenab River flows northwest for approximately 30 km, while the Ravi River flows south-east for approximately 40 km [36] (Figure 1). During summer, the highest temperature in the city is about 45 °C. While the mean maximum and minimum temperatures are recorded as 39 and 27 °C, respectively. In

the winter, these drop to approximately 17 and 6 °C, respectively, and the average annual rainfall recorded in the district is about 300 mm [37,38].

2.2. Data Acquisition and Image Processing

To assess the combined effects of land-use and climate change on groundwater, two datasets from 2000 to 2015 were used. These included datasets from remote sensing (i.e., Normalized Difference Built-up Index (NDBI) and Normalized Difference Vegetation Index (NDVI)) and climate data (i.e., temperature and rainfall).

For the five-year intervals of 2000, 2005, 2010, and 2015, satellite images, including Landsat 5 Thematic Mapper (TM) and Landsat 8 (Operational Land Imager (OLI)), were collected for the analysis of NDBI and NDVI indices, as well as to determine the effect of the temporal changes in NDBI and NDVI on groundwater level (GWL) in the Faisalabad district. The temporal resolution of the images is 16 days, and the spatial resolution is 30 m. All images were downloaded from the USGS Earth Explorer website (<http://earthexplorer.usgs.gov>, last accessed: 28 December 2021). The Landsat data were chosen due to their accessibility and quality. Cloud-free images were used for analysis, as illustrated in (Table 1). The data were collected for the pre-monsoon season (March–May) to avoid water reflectance during the monsoon and rice cultivation season (rice crop period requires an ample amount of irrigation for the cultivation) in the study area. Image preprocessing began with layer stacking to create a multispectral image after combining the necessary bands. The images were also calibrated for noise removal [39]. Therefore, each image was radio-metrically corrected by converting the raw digital numbers (DNs) into the top of atmosphere (TOA) reflectance values to enable inter-annual comparisons. After the preparation of the satellite images, all resulting images were clipped with the vector layer of the administrative boundary of the Faisalabad district.

Table 1. Satellite imagery was used for remote sensing analysis.

Satellite	No. of Images	Sensor	Date
Landsat 5	9	TM	March–May 2000
Landsat 5	9	TM	March–May 2005
Landsat 5	9	TM	March–May 2010
Landsat 8	9	OLI	March–May 2015

The annual climatic data for precipitation and temperature variations of the Faisalabad district were acquired from the Pakistan Meteorological Department (<https://www.pmd.gov.pk/>, accessed on 13 September 2021), which were obtained from numerous metrological stations in the region over a period of 15 years. Climatic factors resulting from changes in rainfall are the main factors contributing to groundwater, which may affect the ratio of recharge and discharge of the groundwater table of an area [40]. In addition, to assess GWL changes in the region, annual GWL data from 2000 to 2015 were collected from monitoring wells from the Punjab Irrigation Department of Pakistan (<https://irrigation.punjab.gov.pk/>, accessed on 13 September 2021). Records of more than three hundred wells were reported, from which 48 wells were selected with appropriate records (Figure 1) and were continuously measured throughout the period of 2000–2015.

2.3. Calculation of Vegetation Indices and Built-Up Indices

2.3.1. Normalized Difference Built-Up Index

The built-up index was computed to examine the growth of areas covered by impervious surfaces, such as asphalt and concrete. It was calculated based on the ratio between shortwave infrared and near-infrared bands [41]. The NDBI was assessed using the following equation:

$$\text{NDBI} = \frac{(\text{SWIR1} - \text{NIR})}{(\text{SWIR1} + \text{NIR})} \quad (1)$$

In Equation (1), SWIR1 and NIR are reflectances. For Landsat-5 (TM), SWIR1 is the reflectance measured in band 5 at wavelength $\lambda = 1.55 - 1.75 \mu\text{m}$, and NIR is the reflectance measured in band 4 at $\lambda = 0.76 - 0.90 \mu\text{m}$. In Landsat-8 (OLI), SWIR1 is the reflectance measured in band 6 at $\lambda = 1.56 - 1.65 \mu\text{m}$, and NIR refers to the reflectance measured in band 5 at $\lambda = 0.85 - 0.87 \mu\text{m}$.

NDBI values range from -1 to $+1$. Very low values of the NDBI (0.1 and below) correspond to non-urban features (such as a canopy of vegetation), while high values indicate areas covered by impervious surfaces, such as asphalt and concrete.

2.3.2. Normalized Difference Vegetation Index

Vegetation density responds to the plant’s water content. The NDVI derived from digital satellite data corresponded to the density of green vegetation [42,43]. The NDVI reflects vegetation density using multispectral data. The magnitude of NDVI is related to the level of photosynthetic activity for observed vegetation [44]. It is calculated based on the ratio between the near-infrared band and the Red band:

$$\text{NDVI} = \frac{(\text{NIR} - \text{Red})}{(\text{NIR} + \text{Red})} \tag{2}$$

here, in Equation (2), NIR and Red, are reflectances. For Landsat-5 (TM), NIR is the reflectance measured in band 4 at a wavelength $\lambda = 0.76 - 0.90 \mu\text{m}$, and Red is the reflectance measured in band 3 with $\lambda = 0.63 - 0.69 \mu\text{m}$. In Landsat 8 (OLI), NIR is the reflectance measured in band 5 at $\lambda = 0.85 - 0.87 \mu\text{m}$, and Red refers to the reflectance measured in band 4 at $\lambda = 0.64 - 0.67 \mu\text{m}$. Areas with a high vegetation index represent intensive vegetation owing to the high NIR reflectance compared with that of visible light (VIS). Table 2 lists the vegetation and urban indices that were tested for their potential to predict the impact on groundwater. Groundwater level related to both NDBI and NDVI was then investigated to clarify any potential effects on GWL.

Table 2. NDBI and NDVI indices for 2000, 2005, 2010, and 2015.

Index Name	Name	Formulation (Landsat 5)	Formulation (Landsat 8)	References
NDVI	Normalized Difference Vegetation Index	$\frac{(\text{NIR} - \text{Red})}{(\text{NIR} + \text{Red})}$	$\frac{(\text{NIR} - \text{Red})}{(\text{NIR} + \text{Red})}$	[45,46]
NDBI	Normalized Difference built-up Index	$\frac{(\text{SWIR1} - \text{NIR})}{(\text{SWIR1} + \text{NIR})}$	$\frac{(\text{SWIR1} - \text{NIR})}{(\text{SWIR1} + \text{NIR})}$	[47]

2.4. Statistical Analysis

We used Pearson’s correlation coefficient (r) to assess the relationship of GWL with NDVI and NDBI indices, climatic parameters of annual temperature, and precipitation to characterize the effect on GWL in the district through a set of independent pixel values chosen from a classified image within the entire study area. The average values for the three months (March to May) of the year 2000, 2005, 2010, and 2015 were calculated by using the cell statistic tool in ArcGIS 10.5. The statistical relationship was implemented in the Origin 2021 (9.8) software package.

2.5. Spatial Interpolation of Groundwater Level Data

Data for un-monitored locations were estimated by applying geo-statistical interpolation methods to the available GWL data. Inverse Distance Weighting (IDW) is a widely used interpolation method [48,49] for distributed point data of groundwater level mapping. IDW is an interpolation method by which unknown values at certain locations can be calculated by linearly combining values at known locations [50,51]. In this study, IDW was applied to investigate the spatiotemporal variation of the average groundwater levels of the year 2000, 2005, 2010 and 2015.

The IDW involves the use of the following equation:

$$Z_{(S_0)} = \sum_{i=1}^N \lambda_i Z_{(S_i)} \tag{3}$$

where (S_0) is the set of sampling points in the search neighborhood of (S_i) , and N is the number of sample points around the prediction point to be used in the prediction calculation process; λ_i is the weight of each sample point to be used in the prediction calculation process, whose value decreases as the distance between the sample point and the prediction point increases; $Z_{(S_0)}$ is the prediction at (S_0) ; and $Z_{(S_i)}$ is the measured value obtained at (S_i) . The interpolation was conducted using ArcGIS 10.5.

2.6. Mann–Kendall Test

The non-parametric Mann–Kendall test is widely used for detecting trends in meteorology and hydrology [52]. The Mann–Kendall trend test [53,54] is based on the correlation between the ranks and sequences of time series. The test statistic (R) of the annual average GWL time series ($x_1, x_2, x_3 \dots$, and x_n) could be calculated using the Mann–Kendall test as:

$$R = \sum_{k=1}^{n-1} \sum_{j=k+1}^n \text{Sign}(x_j - x_k) \tag{4}$$

where n is the number of data points, and x_j and x_k denote the data points of time j and k , respectively:

$$\text{Sign}(x_j - x_k) = \begin{cases} +1, & \text{if } x_j - x_k > 0 \\ 0, & \text{if } x_j - x_k = 0 \\ -1, & \text{if } x_j - x_k < 0 \end{cases} \tag{5}$$

Studies [53,54] have previously documented that the R statistic is approximately normally distributed when $n \geq 8$, with the mean and the variance of test statistics $\text{VAR}(R)$, being estimated as:

$$\text{VAR}(R) = \frac{1}{18} \{n(n-1)(2n+5) - \sum_{i=1}^g t_i(t_i-1)(2t_i+5)\} \tag{6}$$

where g denotes the tied group’s number, which is a set of sample data with similar values and t_i indicates the extent of i th ties. The estimated S and $\text{VAR}(R)$ can be used to estimate the test statistic Z when n is >10 [55]:

$$Z = \begin{cases} \frac{s-1}{\sqrt{\text{VAR}(R)}}, & \text{if } S > 0 \\ 0, & \text{if } S = 0 \\ \frac{S+1}{\sqrt{\text{VAR}(R)}}, & \text{if } S < 0 \end{cases} \tag{7}$$

The standardized Mann–Kendall statistic Z follows a standard normal distribution with $E(Z) = 0$ and $V(Z) = 1$. Positive and negative values of Z specify the direction of trends, with positive values indicating an increasing trend and vice versa.

2.7. Sen’s Slope Estimator

Sen’s slope [56] estimator was used to estimate the magnitude of change in GWL (slope Q). The slope Q could be obtained from N pairs of data as:

$$Q_i = \frac{x_k - x_j}{k - j}, \quad i = 1, 2, \dots, N, \quad k > j \tag{8}$$

where x_k and x_j represent the values of data at k and j times, respectively, and Q_i is the median slope.

3. Results

3.1. Spatial Patterns of Vegetation and Built-Up Indices

The spatial distributions of NDVI for three months (March–May) over the study period (2000, 2005, 2010, and 2015) are shown in (Figure 2). The results show that the three-month average (March–May) vegetation cover over the 15 years decreased gradually. The maximum NDVI values were higher in 2000 than those in 2015, with maximum average NDVI values of 0.31, 0.29, 0.26, and 0.19 in 2000, 2005, 2010, and 2015, respectively.

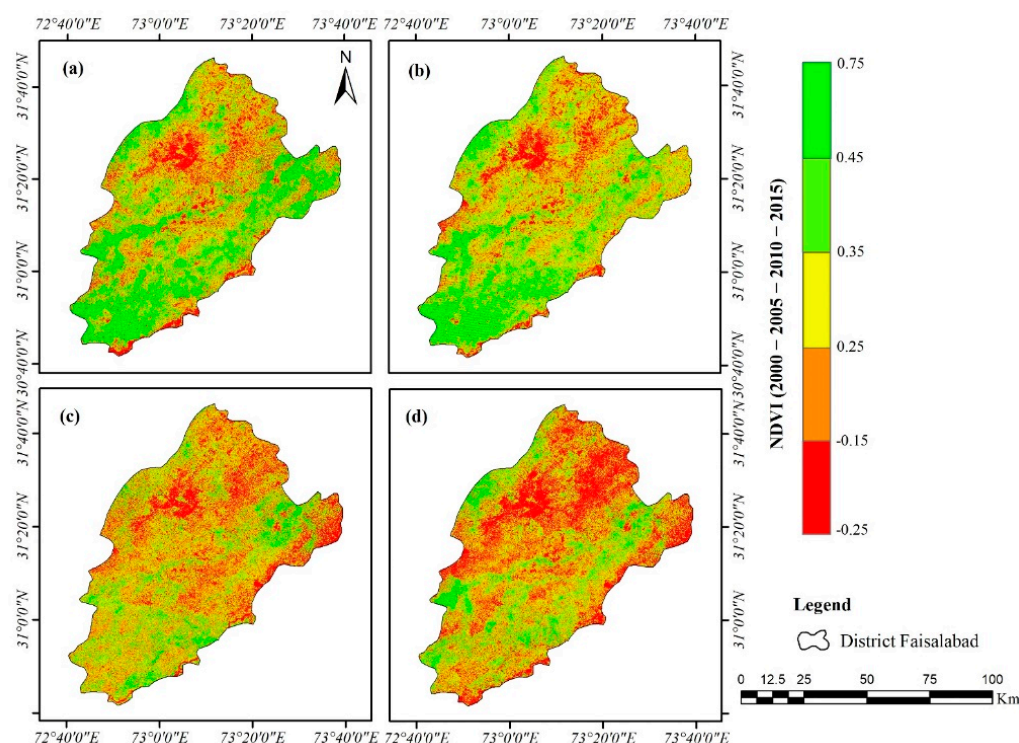


Figure 2. Spatial patterns of normalized difference vegetation index averaged over 3 months (March–May), for 2000 (a), 2005 (b), 2010 (c), and 2015 (d).

The study confirmed that the central areas of the Faisalabad district exhibited low NDVI values and that they increased when moving away from the central area of the district. This was because of the increasing number of buildings and impervious surface expansion. The vegetation cover declined with an increase in built-up area.

The spatial distribution of NDBI for the three-month average (March–May) is shown in (Figure 3). The maximum NDBI values increased from 0.19 in 2000 to 0.51 in 2015. For the years investigated (2000, 2005, 2010, and 2015), the average maximum values of NDBI were -0.14 , -0.10 , -0.07 , and -0.05 , respectively.

The highest NDBI values were observed in the central part and northeast area of the district, such as Lyallpur, Jinnah, Iqbal Madina, and Chak Jhumra towns at each time-point because of the densely built-up areas. These are all towns that continuously expanded into their surroundings over time (Figure 3). The lowest NDBI values were observed in the southwestern part of the district, such as Sammundri, Jaranwala, and Tandlianwala towns, where most areas are cultivated farmland.

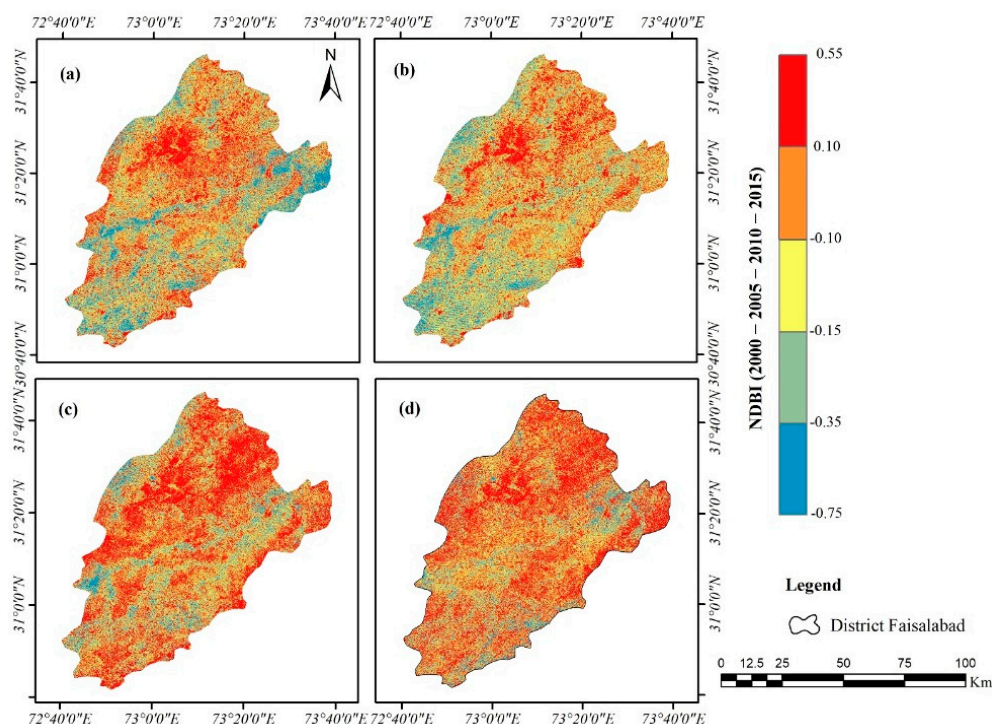


Figure 3. Spatial patterns of normalized difference built-up index averaged over 3 months (March–May), for 2000 (a), 2005 (b), 2010 (c), and 2015 (d).

3.2. Relationship of GWL with NDVI, NDBI, and Climate Patterns

The study revealed that most places in the center of the district exhibited low NDVI values, while peripheral areas and places covered with vegetation had high NDVI values (Figure 2). The result indicated that over time the vegetation in the study area has decreased while it has increased in built-up areas, which potentially caused GWL depletion. Conversely, NDBI (Figure 3), was very high in the center of the district and continuously increased over time. This indicates that NDBI is inversely related to GWL depletion since groundwater decreased as the built-up index increased.

However, the study confirmed that the correlation coefficient between GWL and NDBI was positive (Table 3), with a value of $r = 0.69$, indicating that urbanization has a substantial impact on groundwater resources. The study also found a negative correlation between GWL and NDVI (Table 3), with a coefficient of $r = -0.65$. This means that groundwater depletion corresponds to a decrease in vegetation indices and an increase in built-up indices (Figure 4).

Table 3. Statistics of land-use indices and their correlation with depth to water table (DWT).

	Statistics of NDVI and NDBI				Correlation with DWT	
	Minimum	Maximum	Mean	Standard Deviation	Pearson Correlation Coefficient	Significance (p)
NDVI	0.06	0.46	0.26	0.08	0.99	$p < 0.05$
NDBI	-0.22	0.05	-0.08	0.06	-0.79	$p < 0.05$

Hence, as the built-up area increased, which affected the penetration of rainwater into land and also affected the air temperature, this led to the degradation of vegetation and, as a result, affected the recharge of aquifers. The climatic data on temperature and precipitation from 2000 to 2015 showed that the annual mean temperature and precipitation gradually increased in the study area (Figure 5). The maximum annual temperature increased from 24.53 °C in 2000 to 25.02 °C in 2015 (Table 4). This may be because of the

rapid urbanization and the development of textile industries, which are characterized by very high temperatures.

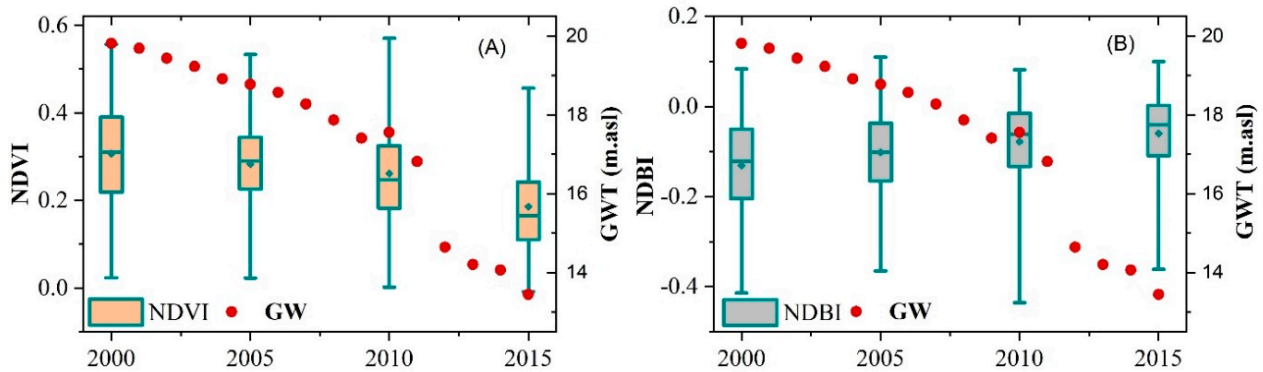


Figure 4. Spatial trend analysis of decreasing groundwater (GW) with NDVI (A) and NDBI (B) over the year 2000, 2005, 2010, and 2015. The whiskers represent the maximum and minimum values of both NDVI and NDBI, and the blue dots are showing the mean values respectively.

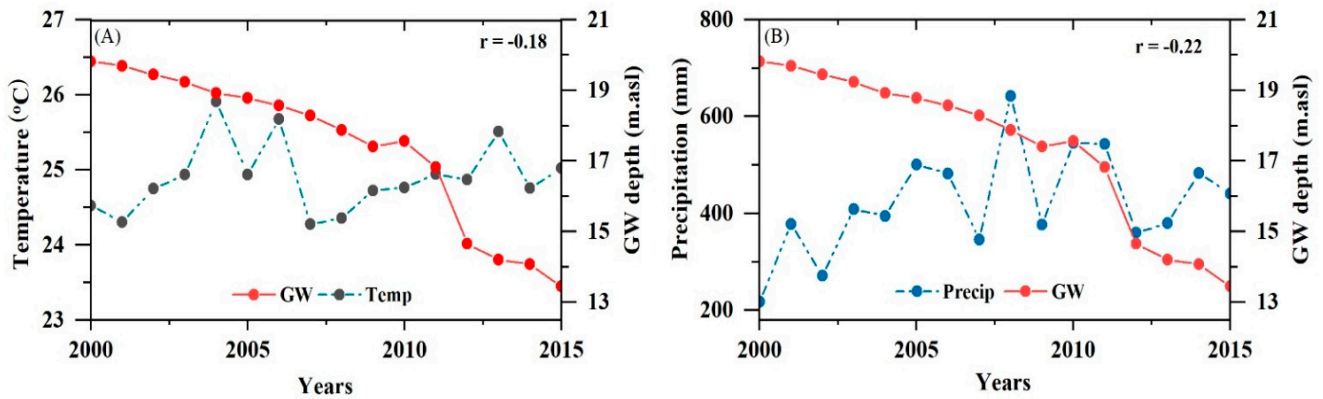


Figure 5. Spatio-temporal trend analysis of average groundwater trends with temperature (A) and precipitation (B) in 2000–2015.

Table 4. Statistics of climatic factors and their correlation with DWT.

	Minimum	Maximum	Mean	Standard Deviation	Correlation Coefficient	Significance (p)
Temperature (°C)	24.27	25.90	24.89	0.47	−0.18	$p > 0.05$
Precipitation (mm)	217.11	642.42	418.62	106.41	−0.22	$p > 0.05$

Figure 5 shows that a non-significantly negative correlation was observed between temperature and rainfall with GWL, indicating that there was a negative relationship between precipitation and temperature with GWL. This is because the groundwater extraction ratio is higher than the amount of penetration.

3.3. Spatial Characteristics of Groundwater Level

To examine the probable combined effects of land-use indices and climatic conditions on the spatial and temporal variability of the annual average GWL in the years 2000, 2005, 2010, and 2015, 48 monitoring wells were selected in the Faisalabad district (Figure 6). Generally, a clear distinction was observed between the northwest and central regions of the Faisalabad district. Greater groundwater depletion and lower GWL were observed in the central region (Figure 6). These findings might suggest that the central part of the study area, where the population is highly dense, requires more water consumption. It could also be deduced that groundwater depletion has been becoming progressively worse from 2000

to 2015; the average GWL depleted by approximately 1.7 m. Groundwater depletion was thus detected, with all fluctuations showing a similar downward trend.

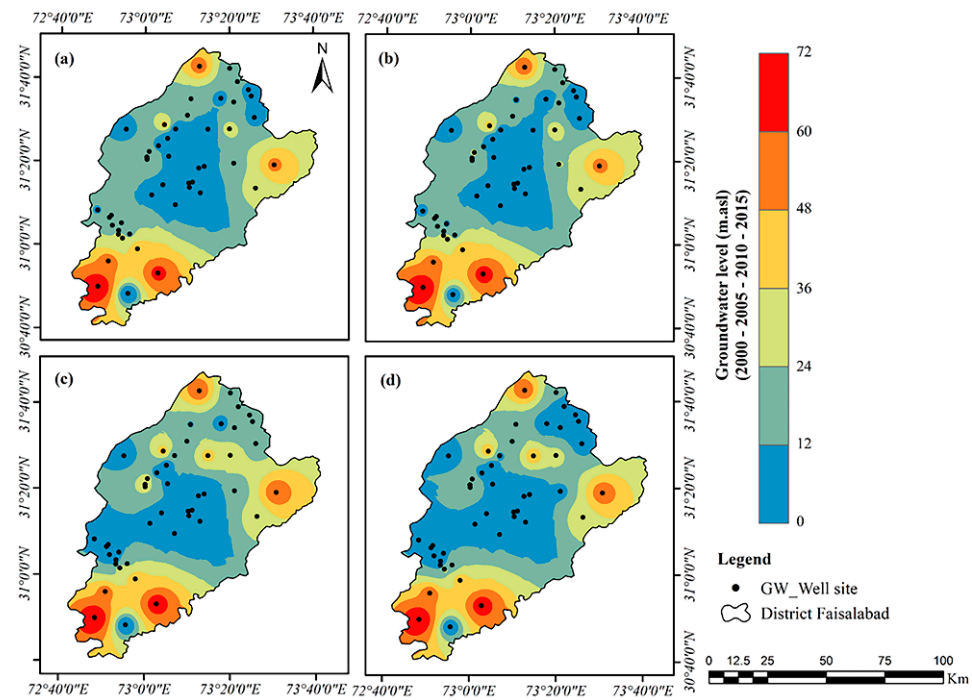


Figure 6. Spatial pattern of annual average groundwater level in 2000 (a), 2005 (b), 2010 (c), and 2015 (d).

3.4. Trends in Groundwater Level

This study investigated the trends in GWL in recent years 2000, 2005, 2010, and 2015 using the Mann–Kendall test and Sen’s slope estimator to assess the magnitude of change in groundwater level. The results in (Figure 7) show that significant decreasing trends were evident for GWL in the Faisalabad district.

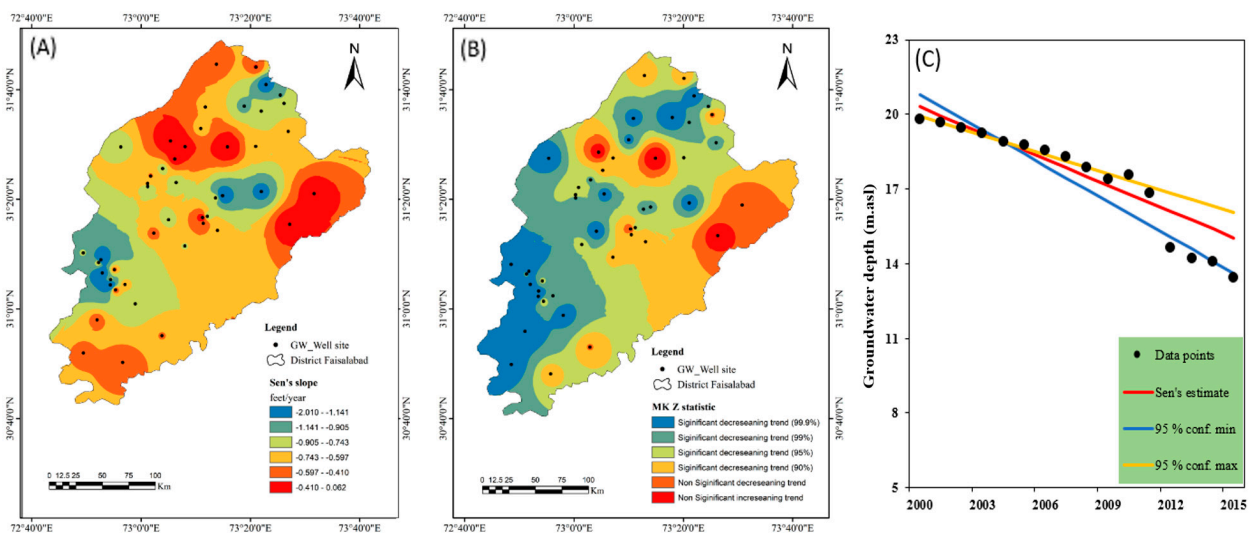


Figure 7. Spatial patterns of groundwater level were estimated using the Mann–Kendall test, showing Sen’s slope (A), Z statistics (B), and the annual average data points (C) from 2000 to 2015.

The results revealed that the overall decreasing trend in GWL obtained from the Sen’s slope in the Faisalabad district was 0.11 m/year. The spatial distribution of the Mann–Kendall test and Sen’s slope of the GWL in most of the studied wells demonstrated

a decreasing tendency (Figure 7A). The spatial distribution of the results of the Mann–Kendall test and Sen’s slope of GWL is presented in (Figure 7B), and most wells showed a significant positive trend (Z statistics) at confidence levels of 95% and 95%, respectively. Furthermore, Z statistics of the Mann–Kendall test indicated that the identified decreasing trends were statistically significant at different confidence intervals.

The results of the Mann–Kendall test and the Sen’s slope estimator on annual temperature and precipitation data from 2000 to 2015 are presented in (Figure 8); the tests indicated increasing trends in all annual climatic parameters. A non-significant ($p > 0.05$) increasing trend at the 95% confidence level was observed in the annual precipitation and temperature series.

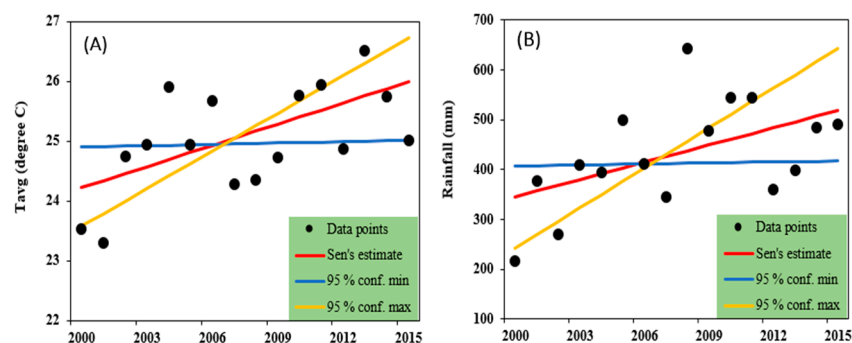


Figure 8. Trend analysis of Mann–Kendall test and Sen’s slope estimator for temperature (A) and precipitation (B) during 2000–2015.

The annual trends of precipitation obtained by the Mann–Kendall test and Sen’s slope estimator are shown in Figure 8B. According to these results, significant increasing trends were observed on the annual scale in the precipitation and temperature series.

4. Discussion

4.1. Relationship of Land-Use and Climate Changes with Groundwater

In recent decades, groundwater has significantly been impacted owing to human activities and climate change. The Faisalabad district is a poorly studied area, and the relationship between land-use and climate changes with groundwater depletion has not been explored comprehensively. The findings indicated that increased built-up area and degradation of vegetation cover led to a considerable impact on GWL in the Faisalabad district. High levels of groundwater exploitation have placed many regions and people at risk, as indicated by the projections of future groundwater resources. Other researchers in different study regions have found a strong relationship between groundwater depletion caused by human actions and land-use change [33,57,58]. For example, Zia et al. [59] investigated the impact of a built-up area on groundwater and revealed that the built-up area in the district is increasing by 36 km² per year, and consequently, the water table is depleting up to 0.14 feet per year.

Land-use changes are not always directly correlated with groundwater depletion but may instead be linked to other factors, such as drought conditions [22]. Our study found that the main threats in the Faisalabad region are from climate change, land-use change, and population growth. In this respect, the application of the Mann–Kendall test and Sen’s slope estimator to the available dataset could determine GWL trends from 2000 and 2015 and also test the applicability of the trends, as GWL datasets are often characterized by missing data over varying time series.

Specific suggestions are presented for achieving more reliable conclusions by assessing the sustainable exploitation of groundwater systems that respond slowly to human and hydraulic stresses. Combined methods are widely used in many environmental fields expressed in continuous area units. This approach is particularly useful because groundwater research is typically conducted using points with inaccurate positions. It is often interesting to detect statistically significant increasing or decreasing trends for indicating human or

climate change effects. Trend testing aims to determine if a specific variable has generally increased or decreased in statistical terms [60]. Previous studies [29,61] have found similar results in different study areas of Mexico, such as the Central Valleys, Oaxaca, Mexico City, Merida, and Yucatan. Other studies on the impact of urbanization have addressed the issue of an increase in groundwater depletion [29,62]. Increased built-up of land owing to increasing population contributes to the reduction in vegetation cover and consequently causes increased evapotranspiration, which contributes to a reduction in soil moisturization. This indicates that land-use change and unplanned urban growth have caused an indirect impact on yield in surrounding areas by changing the amount of groundwater recharge and the water table dynamics. The depletion of groundwater level was observed to be related to the increased built-up area and decreased vegetation cover. Urbanization is thus the primary cause of the depletion in groundwater aquifer recharge rate.

For Faisalabad, this study found the highest groundwater depletion in the central part of the district, particularly in the densely populated area of the city. The influence of the climatic phenomena of annual precipitation and temperature was also assessed, but extreme drought conditions and the aridity index in the region were not considered. These factors are also a potential major cause of groundwater depletion in an area. This study's results contribute to the knowledge of local relationships between climate and land-use change with groundwater. In addition, the degradation of vegetation in the Faisalabad district has intensified in recent years with the increase in built-up areas owing to the unplanned and irregular expansion of built-up areas with industrial and commercial development. From 1980 to 2010, a 40% increase in the total built-up area and a 32% decrease in the non-built-up land was observed in the central part of Faisalabad city [34].

4.2. Future Perspective and Mitigation

The results are consistent with the increased water demand in the last few years, reduced recharge of groundwater stemming from changing land-use, and increasing evapotranspiration owing to an increase in annual temperature and built-up index [63]. Some methods of overcoming these challenges could be strategically protecting recharge zones from urbanization and undertaking small-scale engineering projects.

The recently launched Rain Water Harvesting (RWH) mega project by the Punjab government of Pakistan in the urban area of Lahore [64] is an example of such project. Similar projects should be introduced in other megacities of Pakistan to control the increasing groundwater usage and urban flood control. These projects can also enhance groundwater recharge rates in areas prone to runoff and reduce water consumption rates and pressure on the region's groundwater resources.

This research on the impact of urbanization and climate change on groundwater can be used as a baseline study for the sustainable development of both the urban and agriculture sectors. Local governments and urban planners can use this research for planning the city's long-term growth, especially when determining the influence of groundwater penetration on urban development and reducing the danger of ground surface deformation owing to GWL depletion in the city.

5. Conclusions

Continuous and extreme land-use change and environmental degradation have a particularly damaging effect on regional groundwater resources, both in quality and quantity, in many cities in the world. Therefore, monitoring the effect of land-use and climate changes on groundwater degradation is essential to understanding this trend. In this regard, advanced remote sensing techniques can be used for environmental and land-use monitoring. The result of the present study indicates that from 2000 to 2015, vegetation cover declined and the built-up area increased owing to urban expansion in the Faisalabad district, Pakistan. Meanwhile, the groundwater declined during this period because of the large-scale extraction of groundwater for human activities. This study indicates significant depletion in groundwater related to the transformation of land-use and climate factors in

the Faisalabad district originating from the urbanization process. A positive correlation between NDBI and DWT was observed, whereas negative correlations between DWT and NDVI indicated that the built-up index induced a greater impact on the groundwater recharge process. Vegetation cover has a very significant role in groundwater recharge compared to the built-up area; in areas where vegetation is prevalent, GWL is shallow. The study also indicated that the main threats to groundwater depletion in the Faisalabad district are climate and land-use changes. Variations in mean temperature and precipitation indicate that they might lead to the diminishing recharge of groundwater resources in the future. Increasing temperatures and urbanization enhance evapotranspiration and runoff, leading to a lower potential recharge of aquifers.

Therefore, to mitigate the impact of land-use change on groundwater, city planners and administrators should work on landscape planning approaches from ecological and biodiversity perspectives. The landscape planning of cities should also focus on techniques for regulating the effects of groundwater recharge processes. The policymakers should also ensure an increase in urban green belts and rainwater harvesting mechanisms.

Author Contributions: Conceptualization, M.M.S. and J.W.; methodology and resources, J.W. and M.M.S.; data collection, H.A. and I.U.; software, M.M.S. and F.A.; validation, M.M.S. and R.K.; revised the original manuscript, M.M.S. and J.W. All authors have read and agreed to the published version of the manuscript.

Funding: We thank Yezhi Zhouto for assisting in the review of this manuscript draft. Special acknowledgment should be expressed to the China–Pakistan Joint Research Center on Earth Sciences and the Construction Project of the China Knowledge Center for Engineering Sciences and Technology (Grant number CKCEST-2022-1-41), which supported the implementation of this study.

Institutional Review Board Statement: Not applicable.

Informed Consent Statement: Not applicable.

Data Availability Statement: Not applicable.

Conflicts of Interest: The authors declare no conflict of interest.

References

1. Boretti, A.; Rosa, L. Reassessing the projections of the World Water Development Report. *NPJ Clean Water* **2019**, *2*, 15. [[CrossRef](#)]
2. Döll, P.; Hoffmann-Dobrev, H.; Portmann, F.; Siebert, S.; Eicker, A.; Rodell, M.; Strassberg, G.; Scanlon, B. Impact of water withdrawals from groundwater and surface water on continental water storage variations. *J. Geodyn.* **2012**, *59–60*, 143–156. [[CrossRef](#)]
3. Lytton, L.; Ali, A.; Garthwaite, B.; Punthakey, J.F.; Basharat, S. *Groundwater in Pakistan's Indus Basin: Present and Future Prospects*; World Bank: Washington, DC, USA, 2021; p. 164.
4. Carrard, N.; Foster, T.; Willetts, J. Groundwater as a Source of Drinking Water in Southeast Asia and the Pacific: A Multi-Country Review of Current Reliance and Resource Concerns. *Water* **2019**, *11*, 1605. [[CrossRef](#)]
5. Steinschneider, S.; McCrary, R.; Mearns, L.O.; Brown, C. The effects of climate model similarity on probabilistic climate projections and the implications for local, risk-based adaptation planning. *Geophys. Res. Lett.* **2015**, *42*, 5014–5044. [[CrossRef](#)]
6. Odhiambo, G.O. Water scarcity in the Arabian Peninsula and socio-economic implications. *Appl. Water Sci.* **2016**, *7*, 2479–2492. [[CrossRef](#)]
7. Minnig, M.; Moeck, C.; Radny, D.; Schirmer, M. Impact of urbanization on groundwater recharge rates in Dübendorf, Switzerland. *J. Hydrol.* **2018**, *563*, 1135–1146. [[CrossRef](#)]
8. Dilawar, A.; Chen, B.; Trisurat, Y.; Tuankruea, V.; Arshad, A.; Hussain, Y.; Measho, S.; Guo, L.; Kayiranga, A.; Zhang, H.; et al. Spatiotemporal shifts in thermal climate in responses to urban cover changes: A case analysis of major cities in Punjab, Pakistan. *Geomat. Nat. Hazards Risk* **2021**, *12*, 763–793. [[CrossRef](#)]
9. Mishra, N.; Sharma, A.K. Groundwater Storage Analysis in Changing Land Use/Land Cover for Haridwar Districts of Upper Ganga Canal Command (1972–2011). In *Lecture Notes in Civil Engineering*; Springer: Berlin/Heidelberg, Germany, 2021; Volume 87, pp. 233–241.
10. Sam, A.S.; Abbas, A.; Padmaja, S.S.; Kaechele, H.; Kumar, R.; Müller, K. Linking Food Security with Household's Adaptive Capacity and Drought Risk: Implications for Sustainable Rural Development. *Soc. Indic. Res.* **2018**, *142*, 363–385. [[CrossRef](#)]
11. Shah, T. Groundwater and human development: Challenges and opportunities in livelihoods and environment. *Water Sci. Technol.* **2005**, *51*, 27–37. [[CrossRef](#)]
12. Thomas, V. Confronting Climate-Related Disasters in Asia and the Pacific. *Rev. Econ.* **2014**, *65*, 121–136. [[CrossRef](#)]

13. Mondal, S.K.; Huang, J.; Wang, Y.; Su, B.; Zhai, J.; Tao, H.; Wang, G.; Fischer, T.; Wen, S.; Jiang, T. Doubling of the population exposed to drought over South Asia: CMIP6 multi-model-based analysis. *Sci. Total Environ.* **2021**, *771*, 145186. [[CrossRef](#)] [[PubMed](#)]
14. Mekonnen, M.M.; Hoekstra, A.Y. Sustainability: Four billion people facing severe water scarcity. *Sci. Adv. Sci. Adv.* **2016**, *2*, e1500323. [[CrossRef](#)]
15. Seo, J.Y.; Lee, S.-I. Integration of GRACE, ground observation, and land-surface models for groundwater storage variations in South Korea. *Int. J. Remote Sens.* **2016**, *37*, 5786–5801. [[CrossRef](#)]
16. Nahib, I.; Ambarwulan, W.; Rahadiati, A.; Munajati, S.; Prihanto, Y.; Suryanta, J.; Turmudi, T.; Nuswantoro, A. Assessment of the impacts of climate and LULC changes on the water yield in the Citarum River Basin, West Java Province, Indonesia. *Sustainability* **2021**, *13*, 3919. [[CrossRef](#)]
17. Scanlon, B.R.; Reedy, R.C.; Stonestrom, D.A.; Prudic, D.E.; Dennehy, K.F. Impact of land use and land cover change on groundwater recharge and quality in the southwestern US. *Glob. Chang. Biol.* **2005**, *11*, 1577–1593. [[CrossRef](#)]
18. Bucton, B.G.B.; Shrestha, S.; Kc, S.; Mohanasundaram, S.; Viridis, S.G.; Chaowiwat, W. Impacts of climate and land use change on groundwater recharge under shared socioeconomic pathways: A case of Siem Reap, Cambodia. *Environ. Res.* **2022**, *211*, 113070. [[CrossRef](#)]
19. Awan, U.K.; Ismaeel, A. A new technique to map groundwater recharge in irrigated areas using a SWAT model under changing climate. *J. Hydrol.* **2014**, *519*, 1368–1382. [[CrossRef](#)]
20. Liu, W.; Bailey, R.T.; Andersen, H.E.; Jeppesen, E.; Nielsen, A.; Peng, K.; Molina-Navarro, E.; Park, S.; Thodsen, H.; Trolle, D. Quantifying the effects of climate change on hydrological regime and stream biota in a groundwater-dominated catchment: A modelling approach combining SWAT-MODFLOW with flow-biota empirical models. *Sci. Total Environ.* **2020**, *745*, 140933. [[CrossRef](#)]
21. Chunn, D.; Faramarzi, M.; Smerdon, B.; Alessi, D.S. Application of an Integrated SWAT-MODFLOW Model to Evaluate Potential Impacts of Climate Change and Water Withdrawals on Groundwater–Surface Water Interactions in West-Central Alberta. *Water* **2019**, *11*, 110. [[CrossRef](#)]
22. Lee, K.S.; Chung, E.-S. Hydrological effects of climate change, groundwater withdrawal, and land use in a small Korean watershed. *Hydrol. Process.* **2007**, *21*, 3046–3056. [[CrossRef](#)]
23. Joshi, S.K.; Gupta, S.; Sinha, R.; Densmore, A.L.; Rai, S.P.; Shekhar, S.; Mason, P.J.; van Dijk, W. Strongly heterogeneous patterns of groundwater depletion in Northwestern India. *J. Hydrol.* **2021**, *598*, 126492. [[CrossRef](#)]
24. Bal, M.; Dandpat, A.K.; Naik, B. Hydrological modeling with respect to impact of land-use and land-cover change on the runoff dynamics in Budhabalanga river basing using ArcGIS and SWAT model. *Remote Sens. Appl. Soc. Environ.* **2021**, *23*, 100527. [[CrossRef](#)]
25. Abdelaziz, K.K.; Nicaise, Y.; Séguis, L.; Ouattara, I.; Moussa, O.; Auguste, K.; Kamagaté, B.; Diakaria, K. Influence of Land Use Land Cover Change on Groundwater Recharge in the Continental Terminal Area of Abidjan, Ivory Coast. *J. Water Resour. Prot.* **2020**, *12*, 431–453. [[CrossRef](#)]
26. Adeleke, O.O.; Makinde, V.; Eruola, A.O.; Dada, O.F.; Ojo, A.O.; Aluko, T.J. Estimation of Groundwater Recharges in Odeda Local Government Area, Ogun State, Nigeria using Empirical Formulae. *Challenges* **2015**, *6*, 271–281. [[CrossRef](#)]
27. Scanlon, B.R.; Keese, K.E.; Flint, A.L.; Flint, L.E.; Gaye, C.B.; Edmunds, W.M.; Simmers, I. Global synthesis of groundwater recharge in semiarid and arid regions. *Hydrol. Process.* **2006**, *20*, 3335–3370. [[CrossRef](#)]
28. Jyrkama, M.I.; Sykes, J.F. The impact of climate change on spatially varying groundwater recharge in the grand river watershed (Ontario). *J. Hydrol.* **2007**, *338*, 237–250. [[CrossRef](#)]
29. Graniel, C.E.; Morris, L.B.; Carrillo-Rivera, J.J. Effects of urbanization on groundwater resources of Merida, Yucatan, Mexico. *Environ. Geol.* **1999**, *37*, 303–312. [[CrossRef](#)]
30. Xia, J.; Wu, X.; Zhan, C.; Qiao, Y.; Hong, S.; Yang, P.; Zou, L. Evaluating the dynamics of groundwater depletion for an arid land in the Tarim Basin, China. *Water* **2019**, *11*, 186. [[CrossRef](#)]
31. Yenehun, A.; Dessie, M.; Nigate, F.; Belay, A.S.; Azeze, M.; Van Camp, M.; Fenetie Taye, D.; Kidane, D.; Adgo, E.; Nyssen, J.; et al. Spatial and temporal simulation of groundwater recharge and cross-1 validation with point measurements in volcanic aquifers with variable 2 topography 3. *Hydrol. Earth Syst. Sci. Discuss.* **2021**, 1–37. [[CrossRef](#)]
32. Adhikari, R.K.; Mohanasundaram, S.; Shrestha, S. Impacts of land-use changes on the groundwater recharge in the Ho Chi Minh city, Vietnam. *Environ. Res.* **2020**, *185*, 109440. [[CrossRef](#)]
33. Ashraf, B.; AghaKouchak, A.; Alizadeh, A.; Baygi, M.M.; Moftakhari, H.R.; Mirchi, A.; Anjileli, H.; Madani, K. Quantifying Anthropogenic Stress on Groundwater Resources. *Sci. Rep.* **2017**, *7*, 12910. [[CrossRef](#)] [[PubMed](#)]
34. Bhalli, M.N.; Ghaffar, A.; Shirazi, S.A. Remote Sensing and Gis Applications for Monitoring and Assessment of the Urban Sprawl in Faisalabad-Pakistan. *Pak. J. Sci.* **2012**, *64*, 203–208.
35. Government of Pakistan, Pakistan Bureau of Statistics. 2017. Available online: <https://www.pbs.gov.pk/content/final-results-census-2017> (accessed on 28 December 2021).
36. Mahmood, K. Transition Urbaine et Structures Familiales au Pakistan, le cas de Faisalabad. Ph.D. Thesis, Université d’Orléans, Orleans, France, 2014.
37. Arshad, A.; Zhang, W.; Zaman, M.A.; Dilawar, A.; Sajid, Z. Monitoring the impacts of spatio-temporal land-use changes on the regional climate of city Faisalabad, Pakistan. *Ann. GIS* **2019**, *25*, 57–70. [[CrossRef](#)]

38. Tariq, A.; Shu, H. CA-Markov chain analysis of seasonal land surface temperature and land use landcover change using optical multi-temporal satellite data of Faisalabad, Pakistan. *Remote Sens.* **2020**, *12*, 3402. [CrossRef]
39. Wald, L.; Ranchin, T.; Mangolini, M. Fusion of Satellite Images of Different Spatial Resolutions: Assessing the Quality of Resulting Images. *Photogramm. Eng. Remote Sens.* **1997**, *63*, 691–699. Available online: <https://hal.archives-ouvertes.fr/hal-00365304> (accessed on 26 April 2020).
40. Manap, M.A.; Sulaiman, W.N.A.; Ramli, M.F.; Pradhan, B.; Surip, N. A knowledge-driven GIS modeling technique for groundwater potential mapping at the Upper Langat Basin, Malaysia. *Arab. J. Geosci.* **2013**, *6*, 1621–1637. [CrossRef]
41. Zha, Y.; Gao, J.; Ni, S. Use of normalized difference built-up index in automatically mapping urban areas from TM imagery. *Int. J. Remote Sens.* **2003**, *24*, 583–594. [CrossRef]
42. Chen, D.; Brutsaert, W. Satellite-Sensed Distribution and Spatial Patterns of Vegetation Parameters over a Tallgrass Prairie. *J. Atmos. Sci.* **1998**, *55*, 1225–1238. [CrossRef]
43. Purevdorj, T.S.; Tateishi, R.; Ishiyama, T.; Honda, Y. Relationships between percent vegetation cover and vegetation indices. *Int. J. Remote Sens.* **1998**, *19*, 3519–3535. [CrossRef]
44. Kidwell, K.B. *NOAA Polar Orbiter Data (TIROS-N, NOAA-6, NOAA-7, and NOAA-8) User Guide*; National Oceanic and Atmospheric Administration: Washington, DC, USA, 1984.
45. Sun, C.; Bian, Y.; Zhou, T.; Pan, J. Using of Multi-Source and Multi-Temporal Remote Sensing Data Improves Crop-Type Mapping in the Subtropical Agriculture Region. *Sensors* **2019**, *19*, 2401. [CrossRef]
46. Sarif, M.O.; Rimal, B.; Stork, N.E. Assessment of changes in land use/land cover and land surface temperatures and their impact on surface Urban heat Island phenomena in the Kathmandu Valley (1988–2018). *ISPRS Int. J. Geo-Inf.* **2020**, *9*, 726. [CrossRef]
47. Ehsan, S.; Kazem, D. Analysis of land use-land covers changes using normalized difference vegetation index (NDVI) differencing and classification methods. *Afr. J. Agric. Res.* **2013**, *8*, 4614–4622. [CrossRef]
48. Varouchakis, E.A.; Hristopoulos, D.T. Comparison of stochastic and deterministic methods for mapping groundwater level spatial variability in sparsely monitored basins. *Environ. Monit. Assess.* **2012**, *185*, 1–19. [CrossRef] [PubMed]
49. Nistor, M.M.; Rahardjo, H.; Satyanaga, A.; Hao, K.Z.; Xiaosheng, Q.; Sham, A.W.L. Investigation of groundwater table distribution using borehole piezometer data interpolation: Case study of Singapore. *Eng. Geol.* **2020**, *271*, 105590. [CrossRef]
50. Gunarathna, M.H.J.P.; Kumari, N.; Kumari, M.K.N.; Nirmanee, K.G.S. Evaluation of Interpolation Methods for Mapping pH of Groundwater Assessment and Modeling of Water Resources in Tank Cascade Landscape View Project Evaluation of Interpolation Methods for Mapping pH of Groundwater. *Int. J. Latest Technol. Eng. Manag. Appl. Sci.* **2016**, *3*, 1–5. Available online: www.ijltemas.in (accessed on 25 December 2021).
51. Keblouti, M.; Ouerdachi, L.; Boutaghane, H. Spatial Interpolation of Annual Precipitation in Annaba-Algeria—Comparison and Evaluation of Methods. *Energy Procedia* **2012**, *18*, 468–475. [CrossRef]
52. Gocic, M.; Trajkovic, S. Analysis of changes in meteorological variables using Mann-Kendall and Sen’s slope estimator statistical tests in Serbia. *Glob. Planet. Chang.* **2013**, *100*, 172–182. [CrossRef]
53. Kendall, M. *Rank Correlation Methods, Book Series, Charles Griffin*; Oxford University Press: Oxford, UK, 1975; Available online: https://scholar.google.com/scholar?hl=en&as_sdt=0%2C5&q=Kendall%2C+M.G.%2C+1975.+Rank+Correlation+Methods.+Griffin%2C+London%2C+UK.&btnG=#d=gs_cit&u=%2Fscholar%3Fq%3Dinfo%3AhR1fFHYqYHQJ%3Ascholar.google.com%2F%26output%3Dcite%26scirp%3D1%26hl%3Den (accessed on 27 December 2021).
54. Mann, H.B. Nonparametric Tests Against Trend. *Econometrica* **1945**, *13*, 245–259. [CrossRef]
55. Gilbert, R.O. Statistical Methods for Environmental Pollution Monitoring. *Biometrics* **1988**, *44*, 319. [CrossRef]
56. Sen, P.K. Estimates of the Regression Coefficient Based on Kendall’s Tau. *J. Am. Stat. Assoc.* **1968**, *63*, 1379–1389. [CrossRef]
57. Joodaki, G.; Wahr, J.; Swenson, S. Estimating the human contribution to groundwater depletion in the Middle East, from GRACE data, land surface models, and well observations. *Water Resour. Res.* **2014**, *50*, 2679–2692. [CrossRef]
58. Veldkamp, T.I.E.; Wada, Y.; Aerts, J.; Döll, P.; Gosling, S.N.; Liu, J.; Masaki, Y.; Oki, T.; Ostberg, S.; Pokhrel, Y.; et al. Water scarcity hotspots travel downstream due to human interventions in the 20th and 21st century. *Nat. Commun.* **2017**, *8*, 15697. [CrossRef] [PubMed]
59. Zia, S.; Nasar-u-Minallah, M.; Tahir, M.; Hanif, A. Impact Assessment of Urban Built-Up Area on Groundwater Level of District Faisalabad, Pakistan. *Environ. Geol.* **2022**, *12*, 32–37. [CrossRef]
60. Partal, T.; Kahya, E. Trend analysis in Turkish precipitation data. *Hydrol. Process.* **2006**, *20*, 2011–2026. [CrossRef]
61. Ojeda Olivares, E.A.; Sandoval Torres, S.; Belmonte Jimenez, S.I.; Campos Enriquez, J.O.; Zignol, F.; Reygadas, Y.; Tiefenbacher, J.P. Climate Change, Land Use/Land Cover Change, and Population Growth as Drivers of Groundwater Depletion in the Central Valleys, Oaxaca, Mexico. *Remote Sens.* **2019**, *11*, 1290. [CrossRef]
62. Wakode, H.B.; Baier, K.; Jha, R.; Azzam, R. Impact of urbanization on groundwater recharge and urban water balance for the city of Hyderabad, India. *Int. Soil Water Conserv. Res.* **2018**, *6*, 51–62. [CrossRef]
63. Heerspink, B.P.; Kendall, A.D.; Coe, M.T.; Hyndman, D.W. Trends in streamflow, evapotranspiration, and groundwater storage across the Amazon Basin linked to changing precipitation and land cover. *J. Hydrol. Reg. Stud.* **2020**, *32*, 100755. [CrossRef]
64. Hameed, R.; Javed, M.; Nawaz, M.S. An assessment of adoption of rainwater harvesting system in residential buildings in Lahore, Pakistan. *Urban Water J.* **2020**, *18*, 163–172. [CrossRef]